

Atmósfera (1991), 4, pp. 3–22

On resolution in atmospheric numerical models and cascade processes

A. WIIN-NIELSEN

Geophysical Institute, University of Copenhagen, Denmark

(Manuscript received April 24, 1990; accepted June 20, 1990)

RESUMEN

Se revisan las implicaciones de los procesos en cascada en los modelos barotrópicos y cuasi-geostróficos, usando la conservación de energía cinética y enstrofia en el caso barotrópico y conservación de la suma de energía potencial y cinética disponible, y de enstrofia potencial cuasi-geostrófica en el caso baroclínico.

El límite superior para las cascadas de energía a través de un número de onda esférico dado, obtenido del teorema de Fjørtoft, es usado en el caso barotrópico para estimar la resolución necesaria para impedir casi todas las cascadas a través del máximo número de onda en el espectro computacional.

La generalización a modelos baroclínicos cuasi-geostróficos da la posibilidad de estimar las resoluciones horizontales y verticales requeridas para que, en la resolución computacional, se limite la cascada de energía total, a través del máximo número de onda esférico y tri-dimensional, a una fracción pequeña de la energía total inicial.

ABSTRACT

The implications of cascade processes in barotropic and quasi-geostrophic models are reviewed using conservation of kinetic energy and enstrophy in the barotropic case and conservation of the sum of available potential and kinetic energy and of potential, quasi-geostrophic enstrophy in the baroclinic case. The upper limit for energy cascades across a given spherical wave number, obtained from Fjørtoft's theorem, is in the barotropic case used to estimate the resolution necessary to prevent almost all cascades across the maximum wave number in the computational spectrum.

The generalization to quasi-geostrophic, baroclinic models gives the possibility to estimate the horizontal and vertical resolutions required to limit the cascade of total energy across the maximum three-dimensional, spherical wave number in the computational resolution to a small fraction of the initial total energy.

1. Introduction

In an important paper on atmospheric spectral dynamics Fjørtoft (1953) investigated the energy and enstrophy exchanges in two-dimensional, non-divergent flow. The major tools were the two conservation theorems for this type of atmospheric flows, i.e. the conservations of kinetic energy and enstrophy. The major result was the establishment of an upper limit to the amount of kinetic energy which can be cascaded to small scales. It was also stressed in the investigation that a fundamental difference exists between two- and three- dimensional flows in this regard because truly three-dimensional flows permit the cascade processes to smaller and smaller scales.

It has been pointed out by Charney (1973) that an intermediate case is the one of quasi-geostrophic flow. Two conservative quantities exist for this type of flow, i.e. the conservation of quasi-geostrophic enstrophy and the sum of available potential and kinetic energy. An important

restriction applies in this case, because the latter conservation theorem is true only in the case where the temperature gradient vanishes at the surface of the Earth. However, if this were the case a complete analogy would exist between quasi-geostrophic and two-dimensional, non-divergent flow.

In addition to the general statement on cascade processes Fjørtoft (1953) considers also the special case of a low order system consisting of three components. He points out that under conservation of kinetic energy and enstrophy a change in the kinetic energy on the middle scale will produce changes of the opposite sign on the small and on the large scale. In addition, he maintains that the change in the kinetic energy on the large scale is larger than the change on the small scale. This widely quoted statement is not true in general as we shall demonstrate.

On the other hand, studies based on observations seem to agree with the postulated theorem. Early studies by Saltzman and Fleisher (1960), Saltzman and Teweles (1964) and Yang (1967) are based on a decomposition in longitudinal wave numbers, while a later study by Chen and Wiin-Nielsen (1978) uses a resolution in spherical harmonic functions. The study by Steinberg *et al.* (1971) includes also the nonlinear interactions of enstrophy and potential enstrophy. All these studies show that the kinetic energy is exported from the middle scale to both the larger and the smaller scales with the larger amounts going to the larger scales. The question is as usual how the empirical studies can be understood in terms of the present theory.

In the remaining part of this paper we shall discuss Fjørtoft's theorem and relate it to the observational studies. Some remarks will also be made concerning quasi-geostrophic, baroclinic flow.

2. Nondivergent, horizontal flow

Let us start by considering the two conservation theorems. Developing the stream function as a series of spherical harmonic functions we can express the total kinetic energy and the total enstrophy as infinite series. If n is the meridional index of the associated Legendre functions it turns out that when we write the kinetic energy in the form

$$K = \sum_{n=1}^{\infty} K(n) \quad (2.1)$$

we get the series for enstrophy as follows:

$$a^2 E = \sum_{n=1}^{\infty} c(n) K(n) \quad (2.2)$$

where a is the radius of the Earth and

$$c(n) = n(n+1) \quad (2.3)$$

Considering next a low order system of three components it is important to note that only

components which satisfy the selection rules of Platzman (1960) are of interest because all other components have a vanishing interaction coefficient. Let m be the longitudinal index of the associated Legendre functions. The selection rules are then for three components

$$m_3 = m_1 + m_2$$

$$n_2 - n_1 < n_3 < n_1 + n_2$$

$$n_1 + n_2 + n_3 \quad \text{is odd} \quad (2.4)$$

when it has been assumed that $n_1 < n_2 < n_3$.

(2.1) and (2.2) are for the three component system

$$K_1 + K_2 + K_3 = K$$

$$c_1 K_1 + c_2 K_2 + c_3 K_3 = a^2 E \quad (2.5)$$

It is straightforward to calculate the changes ΔK_1 and ΔK_3 corresponding to a given change on the middle component ΔK_2 . We find that

$$\Delta K_1 = -\frac{c_3 - c_2}{c_3 - c_1} \Delta K_2; \quad \Delta K_3 = -\frac{c_2 - c_1}{c_3 - c_1} \Delta K_2$$

$$\frac{\Delta K_1}{\Delta K_3} = \frac{c_3 - c_2}{c_2 - c_1} \quad (2.6)$$

It is obvious that $\Delta K_1/\Delta K_3$ is positive. To gain insight into the magnitude of the energy ratio we notice that it is larger than unity if

$$c_2 < \frac{1}{2}(c_1 + c_3) \quad (2.7)$$

but it is possible to obey the selection rules and select components in such a way that (2.7) is not satisfied. It was decided to consider a truncation at $n_{\max} = 25$ and to compute the last ratio in (2.6) for all selection rules (2.4). We still get a large number of "active" triplets. (2.7) shows that if n_2 is selected close to n_3 it is unlikely the inequality will be satisfied, while selecting n_2 close to n_1 increases the likelihood that (2.7) will be satisfied. It is not practical to show all values of the ratio, but to illustrate the remarks made above we may first consider Fig. 1 where the ratio $\Delta K_1/\Delta K_3$ is plotted for all active triplets as a function of n_3 with $n_2 = n_3 - 1$. Since n_2 and n_3 have different parity it follows that n_1 must be even. As expected we find that the great majority of the values of the ratio are less than unity. To be exact, only the triplets of the form $(n, n + 1, n + 2)$ produce a value larger than unity. Close to the other extreme we may consider Fig. 2 in which $n_2 = n_3 - 7$. In this case the ratio is larger than one for all active triplets. For the whole sample of triplets it turns out that the majority produces a ratio smaller than unity.

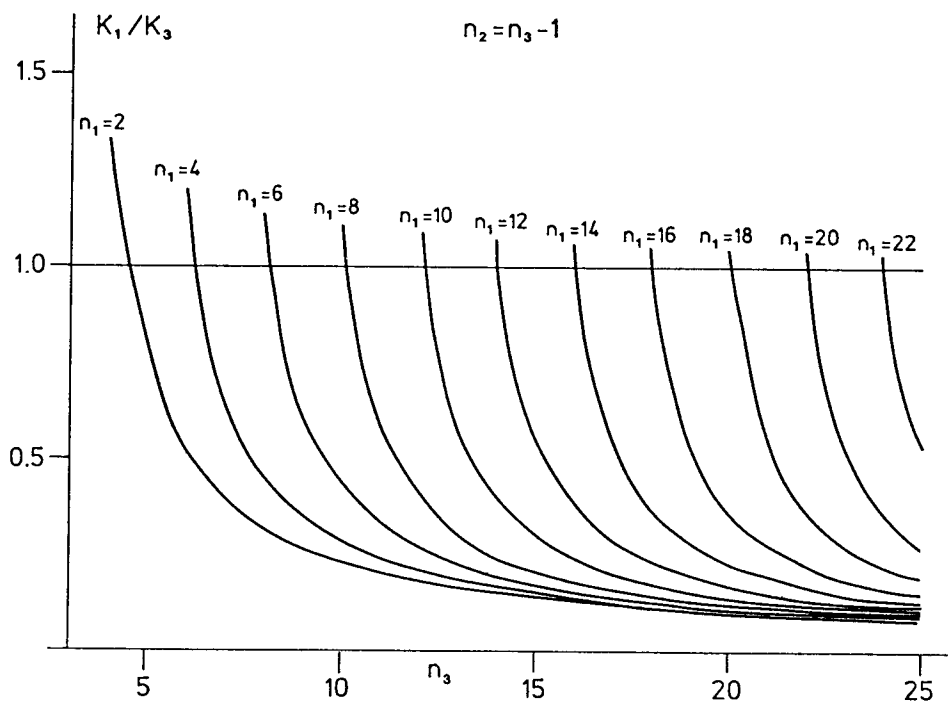


Fig. 1. The ratio K_1/K_3 as a function of n_3 computed for $n_1 = 2, 4, \dots, 22$ and with $n_2 = n_3 - 1$. Only the triplets of the form $(n, n + 1, n + 2)$ result in a value of $K_1/K_3 > 1$.

In view of these results for the basic triplets which together make up the whole set of interactions it is pertinent to ask why the observations seem to agree with Fjørtoft's conclusion. The reason is the way in which the results are presented in all cases. For a given truncation the wave numbers, included in the calculations, are divided in three groups normally called the large, the middle and the small scales. This means that we consider only three groups of waves. For each group we may calculate the amount of kinetic energy represented by the group and an average scale. For a group including all wave numbers from n' to n'' , inclusive, we find

$$K(n', n'') = \sum_{n=n'}^{n''} K(n) \quad (2.8)$$

and the average scale c from the equation

$$cK(n', n'') = \sum_{n=n'}^{n''} c(n)K(n) \quad (2.9)$$

To use (2.8) and (2.9) it is necessary to have a spectrum of kinetic energy as a function of n . In the following we use a spectrum based on the data from three months, January 1983-85, inclusive. For each month the spectrum was divided in two parts: the stationary part equal to the monthly mean and the transient part which is the deviation from the monthly mean. Finally, the spectrum for the stationary waves and for the transient waves were obtained as an average for the three months. The spectrum covers the range $1 \leq n \leq 30$ and were provided by Professor E. Eliassen.

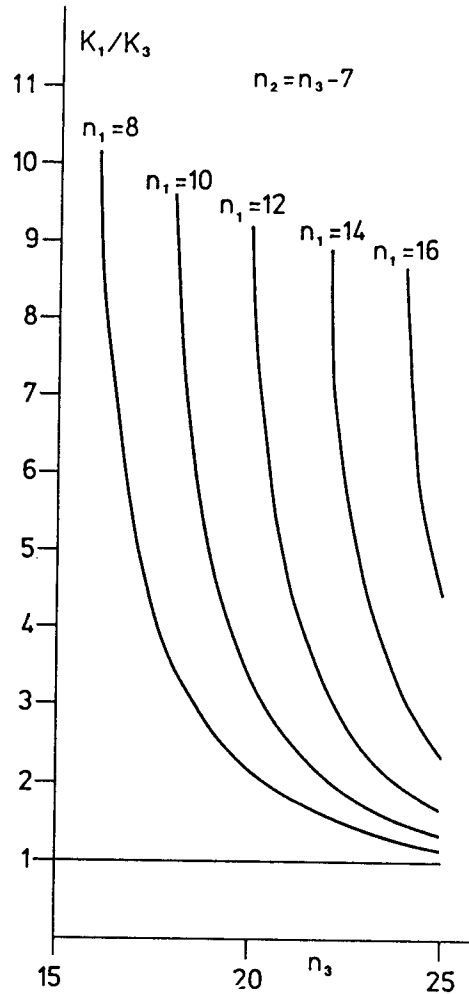


Fig. 2. Arrangement as in Fig. 1, but for $n_1 = 8, 10, \dots, 16$ and $n_2 = n_3 - 7$. Note that all values of K_1/K_3 are larger than unity.

A comparison is first made with the early investigations where a truncation was made at $n = 15$. Dividing the spectrum in three parts, $1 \leq n \leq 5$, $6 \leq n \leq 10$ and $11 \leq n \leq 15$, we find using (2.8) and (2.9) that

$$c_L = 22.64$$

$$c_M = 76.48$$

$$c_S = 174.98$$

and consequently

$$\frac{\Delta K_1}{\Delta K_3} = 1.83; \quad \frac{\Delta E_1}{\Delta E_3} = 0.24$$

in qualitative agreement with the observational studies.

The main aspect of this picture does not change if we use the whole spectrum. In the following example we have used $1 \leq n \leq 10$, $11 \leq n \leq 20$, $21 \leq n \leq 30$ giving

$$c_L = 68.14$$

$$c_M = 221.26$$

$$c_S = 634.73$$

resulting in

$$\frac{\Delta K_1}{\Delta K_3} = 2.70, \quad \frac{\Delta E_1}{\Delta E_3} = 0.29$$

The spectrum can be used also to calculate the upper limit for the energy cascade across a certain wave number as determined by Fjørtoft (1953). For these calculations we need the mean scale for the whole spectrum. It can be obtained from (2.8) and (2.9) setting $n' = 1$ and $n'' = 30$. We find

$$\bar{c} = 177.43$$

From Fjørtoft (*loc.cit*) we note that an upper limit to the fraction of energy which can cascade across $n = N$ is

$$\frac{\sum_{n=N+1}^{\infty} K(n)}{\sum_{n=1}^{30} K(n)} \leq \frac{\bar{c} - c_1}{c_{N+1} - c_1} \quad (2.10)$$

If for example, we want to estimate the upper limit to the cascade across $N = 30$ we find that the right hand side of (2.10) is 0.18. We may also use (2.10) to estimate N in such a way that the energy cascade across $n = N$ is less than r . From

$$\frac{\bar{c} - c_1}{c_{N+1} - c_1} = r \quad (2.11)$$

we find

$$c_{N+1} = \frac{1}{r} [c - (1 - r)c_1] \quad (2.12)$$

Suppose for example that we judge that the observations do not justify a resolution higher than $N = 30$. This does not mean that a prediction based on the data should be limited to $n \leq N$ because the nonlinear processes will cascade the energy to higher wave numbers. The calculation above shows as a matter of fact that a fraction of 0.18 could be cascaded. (2.12) can be used to calculate the prediction range if we want to guarantee that a fraction no larger than r would be cascaded. If we go to the extreme setting $r = 0.01$ we find $c_{N+1} = 17545$ corresponding to a maximum n of about 132. The same argument as above has been applied earlier in a qualitative

sense by Wiin-Nielsen (1985) to explain why an increase in resolution without any better database normally will provide a better forecast. The accuracy of the calculation will naturally depend on the reality of the spectrum which is essential for the whole computation.

3. The quasi-geostrophic baroclinic case

Quasi-geostrophic baroclinic flow is governed by the equation

$$\frac{dQ}{dt} = 0 \quad (3.1)$$

where

$$Q = \eta + \frac{\partial}{\partial p} \left(\frac{f\sigma^2}{\sigma} \frac{\partial \psi}{\partial p} \right), \quad \eta = f + \zeta \quad (3.2)$$

As indicated by (3.1) it has been assumed that the flow is adiabatic and frictionless. Under these circumstances we expect that the sum of available potential and kinetic energy is constant for the domain of the entire Earth. The potential enstrophy is also conserved over the same domain. The change of kinetic energy is:

$$\frac{dK}{dt} = \frac{p_0}{g} \int_0^1 \int_S -\psi \frac{\partial \zeta}{\partial t} ds dp^*, \quad p^* = \frac{p}{p_0} \quad (3.3)$$

The available potential energy is defined by

$$A = \frac{p_0}{2g} \int_0^1 \int_S \frac{f\sigma^2}{\bar{\sigma}p\sigma^2} \left(\frac{\partial \psi}{\partial p^*} \right)^2 ds dp^* \quad (3.4)$$

giving

$$\frac{dA}{dt} = \frac{p_0}{g} \int_0^1 \int_S \left(\frac{\partial \psi}{\partial p^*} \right) \frac{\partial}{\partial t} \left(\frac{f\sigma^2}{\bar{\sigma}p\sigma^2} \left(\frac{\partial \psi}{\partial p^*} \right) \right) ds dp^* \quad (3.5)$$

Integration by parts using the boundary condition that

$$\frac{\partial \psi}{\partial p^*} = 0, \quad p^* = 1 \quad (3.6)$$

gives

$$\frac{dA}{dt} = \frac{p_0}{g} \int_0^1 \int_S -\psi \left[\frac{\partial \partial}{\partial t \partial p^*} \left(\frac{f\sigma^2}{\sigma p_0} \frac{\partial \psi^*}{\partial p^{*2}} \right) \right] ds dp^* \quad (3.7)$$

We have, consequently,

$$\frac{d(K + A)}{dt} = \frac{p_0}{g} \int_0^1 \int_S -\psi \left[\frac{\partial}{\partial t} \left(\zeta + \frac{\partial}{\partial p^*} \left(\frac{f_0^2}{\sigma p_0^2} \frac{\partial \psi}{\partial p^*} \right) \right) \right] ds dp^* \quad (3.8)$$

but using (3.1) we find that the integrand in (3.8) is

$$\psi \vec{v} \cdot \nabla Q = \psi \nabla \cdot (Q \vec{v}) = \nabla \cdot (Q \psi \vec{v}) - Q \cdot \nabla \psi = \nabla \cdot (Q \psi \vec{v}) \quad (3.9)$$

We may thus conclude that $(K + A)$ is conserved in an integral sense. Denoting the relative enstrophy by

$$E = \frac{p_0}{g} \int_0^1 \int_S \frac{1}{2} \xi^2 ds dp^*; \quad \xi = \nabla^2 \psi + \frac{\partial}{\partial p^*} \left(\frac{f_0^2}{\sigma p_0^2} \frac{\partial \psi}{\partial p^*} \right) \quad (3.10)$$

giving

$$Q = f + \xi \quad (3.11)$$

we find after some calculation that

$$\frac{dE}{dt} = \frac{p_0 2\Omega}{g a^2} \int_0^1 \int_S \xi \frac{\partial \psi}{\partial \lambda} ds dp^* \quad (3.12)$$

It turns out that E is conserved under the boundary condition (3.6). To show this we need to consider the integral in (3.12). It vanishes as shown in the Appendix I.

In the following developments we shall express each of the two conservation theorems in wave number space. For each isobaric surface we shall use an expansion in spherical harmonic functions just as in section 2. In addition, it will be necessary for our purposes to find the vertical structure functions which ideally should form a set of normalized, orthogonal functions over the interval from 0 to 1 in the variable p^* . Some degree of freedom exists at this point because the only requirement of the quasi-geostrophic theory is that the static stability parameter should be a function of p only. The specific function is, however, not required.

If we want to cover the whole vertical interval we could, for example, in agreement with Charney (1947) specify an atmosphere with a constant lapse-rate. In that case it has been shown by Jacobs and Wiin-Nielsen (1966) that the vertical structure functions are a set of Bessel functions. Wiin-Nielsen (1989) has discussed this case, and it is possible to define a set which satisfies all the requirements. One may also approach the problem in a different way. It was noticed by Gates (1961) that the static stability parameter

$$\bar{\sigma} = -\alpha \frac{\partial \ln \theta}{\partial p} \quad (3.13)$$

varies approximately as p^{-2} . This observation has been verified using independent data, provided we do not include the very high levels in the atmosphere (say 5kPa and above), in which case $\bar{\sigma}$ varies as $p^{-\delta}$ with δ slightly larger than 2.

The vertical structure functions are, in any case, solutions of the equation

$$\frac{d}{dp^*} \left(\frac{fo^2}{\sigma po^2} \frac{dE_q}{dp^*} \right) + \lambda_q^2 E_q = 0 \quad (3.14)$$

with the boundary conditions $dE_q/dp^* = 0$ at $p^* = 1$ and $p = p_T$, where p_T is a small value of the normalized pressure. We propose to use

$$\sigma = \frac{\sigma_o}{p_*^2} \quad (3.15)$$

in which case (3.14) becomes

$$\frac{d}{dp^*} \left[p_*^2 \frac{dE_q}{dp_*} \right] + \Lambda_q^2 E_q = 0 \quad (3.16)$$

with

$$\Lambda_q^2 = \lambda(q)^2 \frac{\sigma o p o^2}{fo^2} \quad (3.17)$$

One may verify that the required solutions are

$$E_q(p^*) = \left(\frac{2}{(1 + 4\mu(q)^2 \xi_T)} \right)^{\frac{1}{2}} e^{\frac{1}{2}\xi} \left\{ \sin(\mu(q)\xi) - 2\mu(q) \cos(\mu(q)\xi) \right\} \quad (3.18)$$

where

$$\xi = -\ln p^*, \quad \xi_T = -\ln p_T, \quad \mu(q) = \frac{q\Pi}{\xi_T} \quad (3.18)$$

and where the factor in E_q has been determined in such a way that

$$\int_{p_T}^1 E_q(q^*)^2 dp^* = 1 \quad (3.19)$$

It can also be shown that the functions $E_q(p^*)$ are orthogonal, i.e.

$$\int_{p_T}^1 E_q(p^*) E_r(p^*) dp^* = 0, \quad r \neq q \quad (3.20)$$

We note finally that

$$\mu(q)^2 = \Lambda(q)^2 - \frac{1}{4} \quad (3.21)$$

which can be converted to

$$\lambda(q)^2 = \frac{fo^2}{\sigma o p o^2} \left(\frac{1}{4} + \frac{q^2 \Pi^2}{\xi_T^2} \right) \quad (3.22)$$

With these preparations we may write the streamfunction as a triple infinite series

$$\psi(\lambda, \phi, p^*) = \sum_q \sum_m \sum_n \Psi(m, n, q) P_n^m(\phi) e^{im\lambda} E_q(p^*) \quad (3.23)$$

In complete analogy to the nondivergent, horizontal case we get in this case

$$\begin{aligned} K + A &= \frac{p_0}{2g} \sum_q \sum_n \sum_m (s(n)^2 + \lambda(q)^1) \Psi(m, n, q)^2 \\ E &= \frac{p_0}{2g} \sum_q \sum_n \sum_m (s(n)^2 + \lambda(q)^2)^2 \Psi(m, n, q)^2 \end{aligned} \quad (3.24)$$

or writing

$$T(n, q) = (s(n)^2 + \lambda(q)^2) \sum_m \Psi(m, n, q)^2 \quad (3.25)$$

we may write (3.24) in the following way:

$$\begin{aligned} T &= K + A = \frac{p_0}{2g} \sum_q \sum_n T(n, q) \\ E &= \frac{p_0}{2g} \sum_q \sum_n \alpha(n, q)^2 T(n, q) \end{aligned} \quad (3.26)$$

with

$$\alpha(n, q)^2 = s(n)^2 + \lambda(q)^2; \quad s(n)^2 = \frac{n(n+1)}{a^2} \quad (3.27)$$

The numbers $\alpha(n, q)$ may for a given truncation in n and q be arranged as an increasing series. In the following we shall assume that this has been done, and we shall use r as the index for the series so arranged. We may then define the mean scale m^2 by the equation

$$m^2 \cdot \frac{p_0}{2g} \sum_{r=1}^{\infty} T(r) = \frac{p_0}{2g} \sum_{r=1}^{\infty} \alpha(r)^2 T(r) \quad (3.28)$$

We realize of course that in practice all spectra have to be finite. When we nevertheless use an upper limit of infinity it should be understood that $T(r)$ will be essentially zero for sufficiently large values of r . Suppose then that we divide the whole spectrum in two parts: $1 \leq r \leq R$ and $r \geq R + 1$. We may then define two mean scales corresponding to this division as follows

$$\begin{aligned} m_*^2 \sum_{r=1}^R T(r) &= \sum_{r=1}^R \alpha(r)^2 T(r); \quad m_{**}^2 \sum_{r=R+1}^{\infty} T(r) = \\ &= \sum_{r=R+1}^{\infty} \alpha(r)^2 T(r) \end{aligned} \quad (3.29)$$

From (3.28) we note that $m > \alpha(1)$, while (3.29) gives $\alpha_1 < m_* < \alpha(R)$ and $m_{**} \geq \alpha(R_1)$. With these definitions the system (3.26) becomes

$$\begin{aligned} S_1^R + S_{R+1}^\infty &= S_1^\infty \\ m_*^2 S_1^R + m_{**}^2 S_{R+1}^\infty &= m^2 S_1^\infty \end{aligned} \quad (3.30)$$

where

$$S_{r_1}^{r_2} = \sum_{r=r_1}^{r_2} T(r) \quad (3.31)$$

The solution of (3.30) is

$$\frac{S_1^R}{S_1^\infty} = \frac{m_{**}^2 - m^2}{m_{**}^2 - m_*^2}; \quad \frac{S_{R+1}^\infty}{S_1^\infty} = \frac{m^2 - m_*^2}{m_{**}^2 m_*^2} = r \quad (3.32)$$

From the definitions in (3.29) it is clear that

$$m_*^2 < m_{**}^2 \quad (3.33)$$

but since the quantities on the left hand sides of (3.32) are positive it follows also that

$$m_*^2 < m \leq m_{**}^2 \quad (3.34)$$

The second ratio in (3.32) measures the fraction of the total energy contained in the components with $r > R$. This ratio would be unity if $m^2 = m_{**}^2$, but this is possible only if $m^2 > \alpha(R+1)^2$, or, in other words, if we decided to make the division of the spectrum at a very small value of R . We decide not to do that, and we can always guarantee that $m^2 < \alpha(R+1)^2$. We have then

$$\frac{S_{R+1}^\infty}{S_1^\infty} < \frac{m^2 - \alpha(1)^2}{\alpha(R+1)^2 - \alpha(1)^2} < \frac{m^2}{\alpha(R+1)^2} \quad (3.35)$$

where the last inequality holds because $m^2 < \alpha(R+1)^2$.

Using (3.35) it is possible to make some general statements about cascade processes. Suppose for example that it has been decided that the observations permit a resolution no higher than $\alpha(R_A)^2$. Such a decision can be made from diagnostic studies by saying for example that, $r < R_A$ should contain 99% of the total energy. We consider this question in section 4. The initial analysis consists then, in principle, of a spectrum, where significant coefficients in the spectral representation exist for $\alpha < \alpha(R_A)$. For this spectrum it is clear that $m^2 < \alpha(R_A)^2$. Let us next consider the resolution in the model, say $\alpha = \alpha(R_M)$. In general, we would want to use a higher resolution in the model (i.e. $\alpha(R_M) > \alpha(R_A)$) to give room for the cascade processes and thereby prevent an undesirable false accumulation of energy on the highest wave numbers. The value of $\alpha(R_M)$ can be estimated from (3.35) by requiring that

$$\frac{\alpha(R_A)^2 - \alpha(1)^2}{\alpha(R_M)^2 - \alpha(1)^2} < b \quad (3.36)$$

where b should be selected as a reasonably small number. Suppose that R_A corresponds to $n = 30$ and $q = 3$ which means an assumption that waves with a wavelength less than about 1000 km cannot be analysed with accuracy and that three vertical structure functions depict the important vertical scales. We would then have:

$$\alpha(1)^2 = \alpha(0, 1)^2 = 2.64 \times 10^{-12} m^{-2}$$

and

$$\alpha(R_A)^2 = \alpha(30, 3)^2 = 44.20 \times 10^{-12} m^{-2}$$

Setting $b = 0.05$ we find that (3.36) is satisfied if

$$\alpha(R_M)^2 > \alpha(1)^2 + \frac{1}{b}(\alpha(R_A)^2 - \alpha(1)^2) = 8.34 \times 10^{-10} m^{-2}$$

Having this value we enter the ordered table of $\alpha(r)^2$ - value, and we can, of course, find a number which is closest to the estimated value. In this sense the problem has a unique solution.

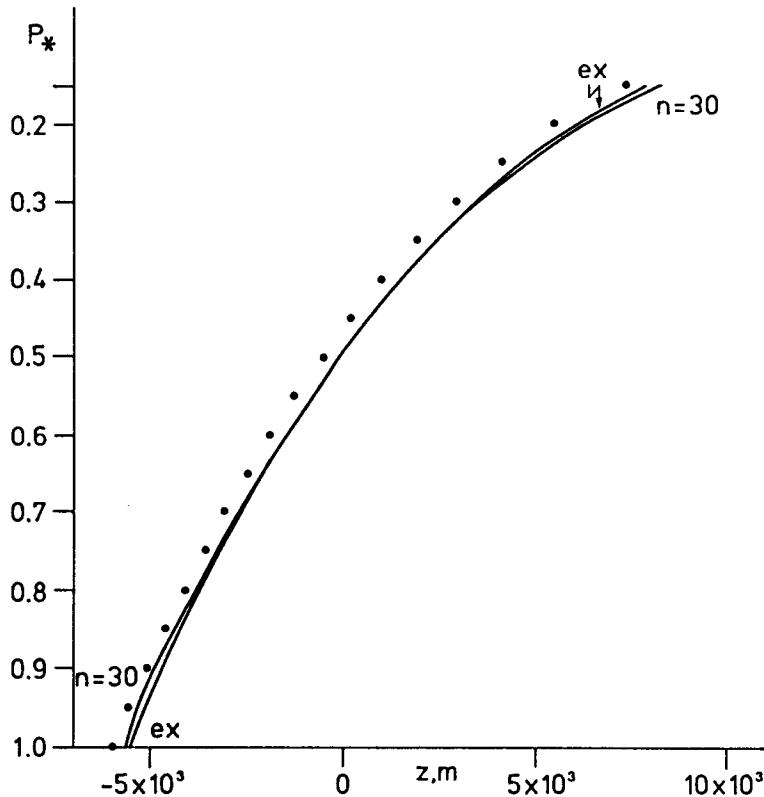


Fig. 3. $Z' = \Phi'/g$ as a function of normalized pressure $p^* = p/p_0$. The curve, marked ex., is obtained from the exact formula, while the curve marked $n = 30$, is obtained from the first 30 vertical components. The dots show the values from the U. S. Standard Atmosphere.

On the other hand, we have provided an inaccurate estimate using (3.36), and we have therefore a number of possibilities, because the value of $\alpha(R_M)^2$ can be approximated by various pairs (n, q) . For example, the following pairs are all in the neighborhood of the estimated value: (112, 15), (98, 16), (80, 17) and (56, 18). Even more extreme cases could be given with small values of n and large values of q or vice versa. The practical solution is normally to determine q separately in such a way that the various parameters are described in a satisfactory way in the vertical direction. Some examples are given in Appendix II and Figures 3 and 4. The estimates given above are based on our knowledge of cascade processes in the atmosphere. We know from diagnostic studies that potential enstrophy is cascaded toward higher wave numbers by nonlinear interactions (Chen and Wiin-Nielsen, 1978) for sufficiently large wave numbers. This process will go on as the forecast is produced by integration of the model equations. This means, considering the definition in (3.29), that m_{**}^2 will increase, while m_*^2 will decrease. (3.35) is then based on the fact that m_*^2 cannot be less than $\alpha(1)^2$, while m_{**}^2 will remain larger than $\alpha(R+1)^2$. It is also seen that these estimates are quite inaccurate. Better estimates can of course be obtained by following the changes in the two mean scales during a forecast. Although such experiments have not been performed, it is to be expected that m_*^2 will not be as small as $\alpha(1)^2$, while m_{**}^2 actually would increase during the integration.

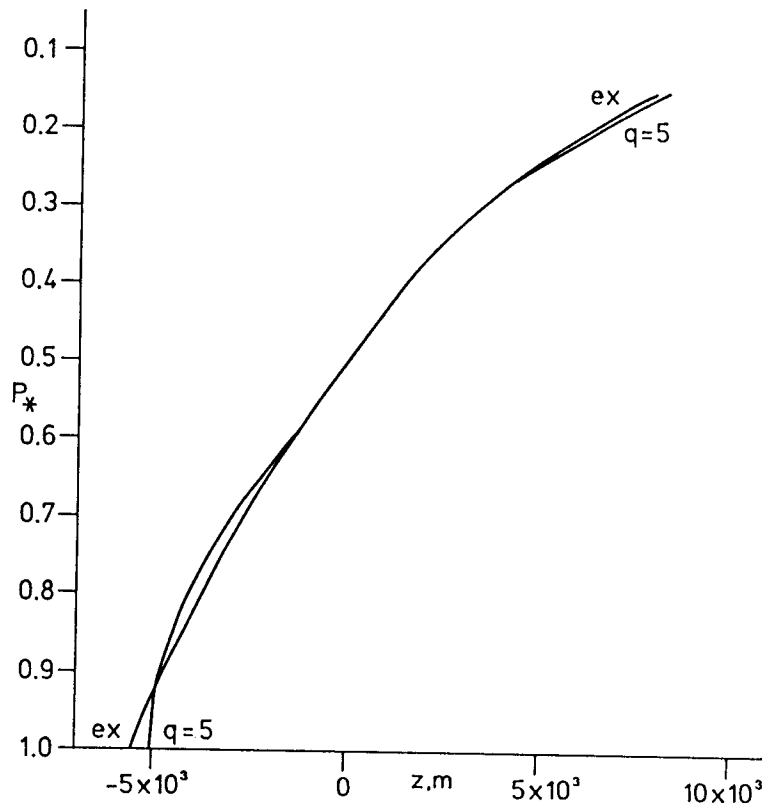


Fig. 4. A comparison of the exact curve, marked ex., and the curve obtained from the first 5 vertical components.

4. An observational study

The purpose of the diagnostic study is to investigate the spectrum of the total energy $A + K$ as discussed in section 3 of this paper. The basic data available for the study were the coefficients in an expansion of the relative vorticity in associated Legendre functions for a number of pressure levels. We denote them $Z(m, n, p^*)$ where m is the longitudinal wave number, n the meridional index and $p^* = p/p_0$, $p_0 = 100$ kPa. For our purpose we need to convert these to vertical structure functions described in the previous section using the formula

$$Z(m, n, q) = \int_{p_T}^1 Z(m, n, p^*) E_q(p^*) dp^* \quad (4.1)$$

where $E_q(p^*)$ is given by (3.18). The levels for p^* were: 0.1, 0.15, 0.20, 0.25, 0.30, 0.40, 0.50, 0.70, 0.85 and 1.00. The integral in (4.1) was evaluated using these levels and the trapezoidal approximation. (3.24) was used to obtain all the terms in the summation leading to $A + K$, noting that

$$\Psi(m, n, q) = \frac{a^2}{n(n+1)} Z(m, n, q) \quad (4.2)$$

It was also decided to obtain $A + K$ as a summation over n and q by defining:

$$S(n, q) = \sum_{m=1}^{m \leq n} z(m, n, q)^2 \quad (4.3)$$

The largest value of n is 63 and that of q is 5.

The calculation of the energy spectrum was carried out once a day, but we shall be concerned mainly with the averaged spectrum for the month. The total averaged amount of energy ($A + K$) turned out to be 3962 KJm^{-2} , and the averaged scale m^2 for the total spectrum is $2.715 \times 10^{-11} m^{-2}$, which very nearly correspond to $n = 15$ and $q = 3$. Another pair ($n = 26$, $q = 2$) is also close to the averaged scale, but we prefer the first pair because the meridional wave number, $n = 15$, is more reasonable considering our knowledge of the spectra as a function of the meridional index n from earlier studies (Chen and Wiin-Nielsen, 1978). The result concerning the averaged scale is perhaps a little surprising at first glance considering that many prediction models had a truncation at $T(15)$ (which means a triangular truncation at $n = 15$) in the early days of global prediction. The explanation is of course that these models were not restricted to $q = 3$ necessarily, and, as we shall see, the addition of the contribution from values of q larger than 3 makes quite a difference.

In interpreting these results we should also have in mind that the averaged scale m^2 is defined (see eq. (3.28)) as the scale which multiplied by the total energy gives the total potential enstrophy. Geometrically speaking we may say that the area of the rectangle with the dimensions of the average scale and the total energy is the same as the area under the curve of potential enstrophy considering all scales. The average scale does not divide the energy or the enstrophy in equal parts.

The next question is how far we will have to go in the spectrum to be sure that we have resolved

the major part of the total energy. We may for example decide that we want to find the value α^2 beyond which we have only 1% of $A + K$. For this purpose we have computed the last ratio in (3.32) which is the ratio of unresolved energy to the total energy. The result is given in Fig. 5 where the ratio r is shown as a function of α , given in the unit of $10^{-6}m$. The curve is of course by definition a decreasing function of α because the addition of an additional value of α in the discrete set will automatically make the numerator S_{R+1}^{∞} smaller while the denominator S_1^{∞} remains the same. Nevertheless, the curve consists of regions, where the slope is very small, followed by a rather abrupt change in r . The first "plateau" around $r = 0.78$ consists of values with $q = 1$ and a few values with $q = 2$ and small values of n . As n increases, retaining $q = 2$, we drop to the next "plateau" around $r = 0.60$. The following almost horizontal level around $r = 0.40$ contains pairs with $q = 3$ and rather large values of n . Another level with $r \simeq 0.22$ contains, in an analogous way, pairs with $q = 4$ and moderately large values of n until the curve falls to almost zero when $q = 5$ and $n = 15$.

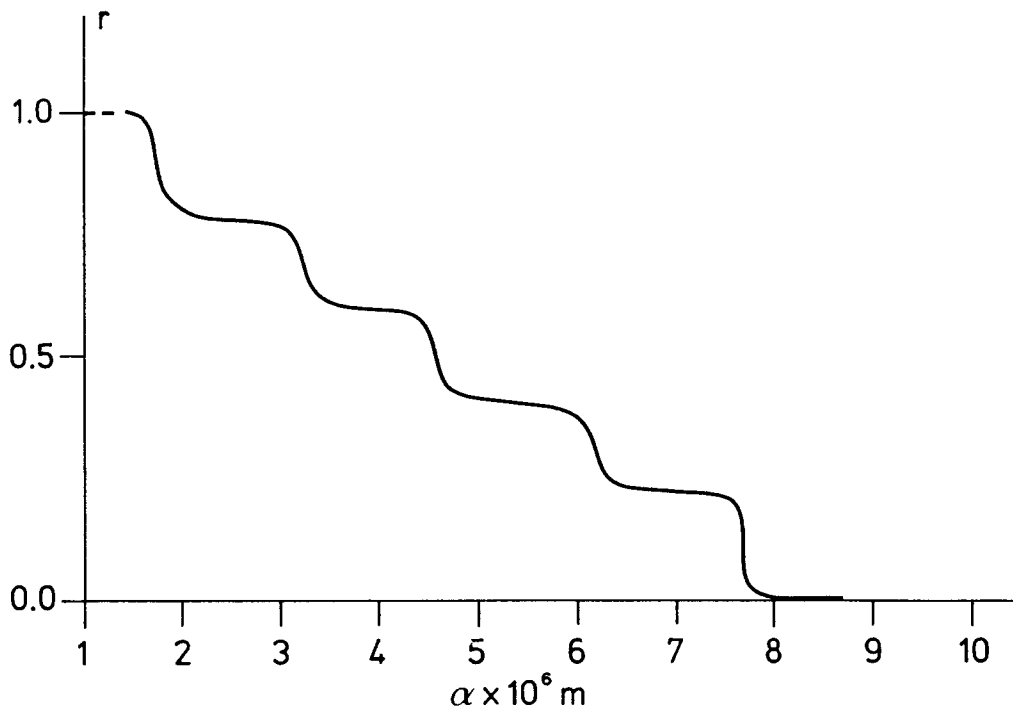


Fig. 5. The ratio of the energy beyond wave number α and the total energy, including all wave numbers, as a function of the wave number α .

From Fig. 5 we then conclude that 99% of the energy $A + K$ is included if we truncate at $n = 15$, $q = 5$. The truncation just mentioned applies of course to the average spectrum for the month. α_A will be the wave number corresponding to $n = 15$ and $q = 5$, indicating that it may correspond to the analysis or initial state. On this basis we proceed to estimate the largest wave number in the model (α_M) following the same procedure as in section 3. With

$$r < \frac{m^2 - \alpha(1)^2}{\alpha(M)^2 - \alpha(1)^2} = e \quad (4.4)$$

we calculate $\alpha(M)^2$ for $m^2 = 2.715 \times 10^{-11} m^{-2}$, $\alpha(1)^2 = 2.689 \times 10^{-12} m^{-2}$ and $e = 0.02$. We have deliberately taken e somewhat larger than the analysis accuracy in view of the poor estimate in (4.4). We find $\alpha(M)^2 = 1225.7 \times 10^{-12} m^{-2}$. The following pairs (n, q) are close to this value

n	q
89	21
109	20
124	19
138	18

We notice that the values of n in the small table above are of the same order of magnitude as those presently used in medium-range weather prediction models. It is more difficult to make comparisons in the vertical direction because the medium-range prediction models normally use gridpoints in the vertical direction and not vertical structure functions. In the data used for the diagnostic study we had 10 information levels. The number of levels in the more advanced prediction models is around 20. With the 10 analysis levels we have judged that a maximum value of $q = 5$ could be justified because $E_5(p^*)$ has 5 zeros and the information levels are closer to each other in the upper atmosphere than in the lower.

Table 1

The zeros of the functions

$E_q(p^*)$ for $q = 1, \dots, 5$.

$q = 1$	$p^* = 0.3699$
$q = 2$	$p^* = 0.6082, 0.1923$
$q = 3$	$p^* = 0.7178, 0.3332, 0.1546$
$q = 4$	$p^* = 0.7799, 0.4385, 0.2466, 0.1387$
$q = 5$	$p^* = 0.8196, 0.5172, 0.3263, 0.2059, 0.1299$

Table 1 shows the position of the zeros of $E_q(p^*)$ for $q = 1, 2, \dots, 5$, while Fig. 6 displays the distribution of $(A + K)$ on the five values of q . In the relatively large value of $(A + K)$ even at $q = 5$ we see an indication that the selected value of the maximum values for q is not large enough because one would expect smaller values of the total energy at this end of the spectrum. In any case, we have provided an estimate of the resolution required to permit the enstrophy cascade to large values of n and q without damage to the prediction.

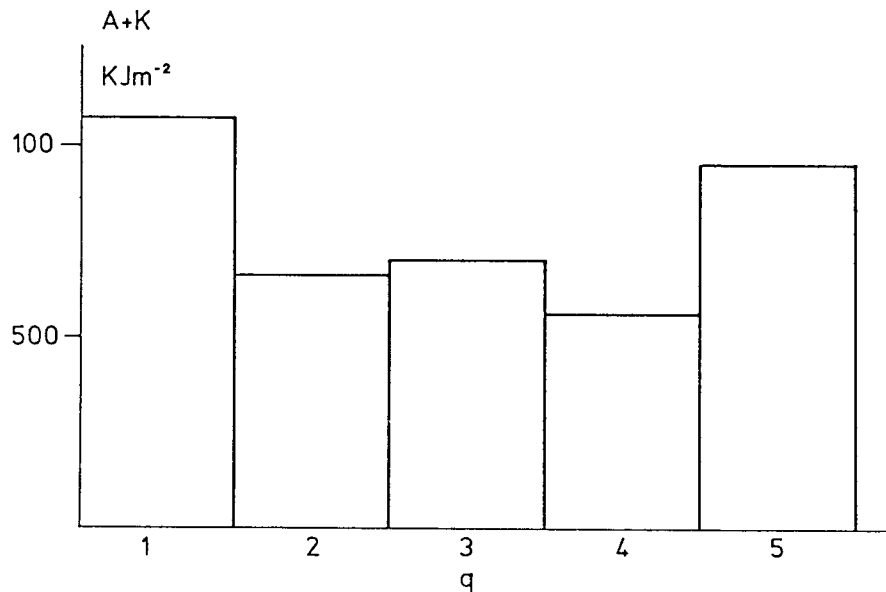


Fig. 6. The total energy for the five first vertical wave numbers.

5. Conclusions

This investigation makes use of the conservation theorems for barotropic and quasi-geostrophic flow to make an estimate of the resolution necessary in prediction models as compared to the resolution in the analysis which is determined by the density and quality of the observations. In the barotropic case the kinetic energy and the enstrophy are conserved in an integrated sense. It follows from the conservation theorems that the cascade processes through nonlinear interactions to smaller scales are limited. An analogous statement can be made for quasi-geostrophic, baroclinic flow where the sum of available potential and kinetic energy, as well as the potential enstrophy are conserved.

It is first demonstrated that an agreement exists between observational and theoretical studies with respect to the nonlinear transfer of kinetic energy through the spectrum, when the whole spectrum is divided in three groups, i.e. the large, the medium and the small scales. It turns out that the mean scales for each of the three groups in practice are separated in such a way that, considering the three groups as if they were individual wave number with a scale equal to the mean scales, the nonlinear interactions will transfer more kinetic energy to the larger than to the smaller scales. This is not necessarily true for three arbitrarily selected wave numbers, as demonstrated in the beginning of the paper.

The estimate of the required resolution in a barotropic prediction as compared to the resolution justified by the data is based on the two conservation theorems which imply that the mean scale is conserved. Dividing the whole spectrum in two parts, called the large and the small scales, we observe that the mean scales of each of the two parts will change systematically during the forecast because the enstrophy is transported across the dividing wave number from the larger to the small scales. The mean scale for the larger scale will thus be smaller while the mean scale for the other part of the spectrum will increase. This principle can be used to make an estimate of a scale across which only a given small fraction of the total can be transferred.

The generalization to quasi-geostrophic, baroclinic flow can be made, realizing that the conservation of kinetic energy is replaced by the conservation of the sum of available potential and kinetic energy, the enstrophy is replaced by the potential enstrophy, and the two-dimensional horizontal scale has a three-dimensional wave number as its analogue. A diagnostic study of the data for January, 1983, providing a division as a function of the three-dimensional wave number, shows that 99% of the total energy is accounted for if the truncation is made at $n = 15$ and $q = 5$. The results of the data study are then used to estimate the necessary truncation in the prediction model.

The estimates are unfortunately not very accurate, but provide a first order of magnitude calculation of required resolutions. An improvement could be made if a number of numerical prediction integrations were performed.

Acknowledgements

The author expresses his appreciation to Professor E. Eliassen for providing the observed spectra used in Section 2, to Mr. Asger Clausen and Mr. Leif Laursen of Denmark's Meteorological Institute for providing the data and programming assistance for the calculation in the diagnostic study.

Appendix 1

We are first required to show that

$$I = \int_s \zeta \frac{\partial \psi}{\partial \lambda} ds = 0 \quad (\text{A.1})$$

In (A.1) we introduce the expressions for the nondivergent meridional wind component and the relative vorticity. We may then write the integral in the form:

$$I = \int_0^{2\pi} \int_{-\pi/2}^{\pi/2} \left(\frac{\partial v}{\partial \lambda} - \frac{\partial u \cos \phi}{\partial \phi} \right) v a^2 d\lambda d\phi \quad (\text{A.2})$$

It is obvious that the first term in this integral vanishes. To evaluate the second term we make use of the fact that the wind is assumed to be nondivergent and it is then seen that also this part integrates to zero.

We are also required to show that the integral

$$J = \int_0^1 \int_s \frac{\partial \psi}{\partial \lambda} \frac{\partial}{\partial p_*} \left(\frac{f_o^2}{\sigma p_o^2} \frac{\partial \psi}{\partial p_*} \right) ds dp_* = 0 \quad (\text{A.3})$$

This can be done by integrating first by parts with respect to p_* , using the upper and lower boundary conditions. Thereafter it is seen that the remaining integral vanishes when integrated with respect to longitude using the cycle condition for this direction.

Appendix 2

The baroclinic case treated in this paper requires a decomposition in spherical harmonic components and in the vertical structure functions. While the first part is done in daily operational numerical forecasts, it may be of interest to consider the vertical decomposition. As an example we consider the spherical harmonic component $m = 0$, $n = 0$ corresponding to the global mean value. Starting from (3.15) we use the definition of the static stability to obtain an equation for the globally averaged geopotential:

$$p_*^2 \frac{d^2 \phi}{dp_*^2} + \frac{c_v}{c_p} p_* \frac{d\phi}{dp_*} = \sigma_o p_o^2 \quad (\text{A.4})$$

The solution to (A.4) satisfying the boundary conditions that $\phi = \phi_o$ and $T = T_o$ at $p_* = 1$ is:

$$\phi = \phi_o - \frac{\sigma_o p_o^2}{\kappa} - \left(\frac{\sigma_o p_o^2}{\kappa^2} - \frac{RT}{\kappa} \right) (1 - p_*^n); n = R/c_p \quad (\text{A.5})$$

From (A.5) we may compute the vertical average over the interval from p_T to 1 and thereafter calculate the deviation from the vertical average.

Fig. 3 shows the deviation from the vertical average from the formula above as well as the curve obtained by computing the first 30 vertical components and recomputing the curve from them. The dots in Fig. 3 indicates the values obtained from the U. S. Standard Atmosphere. The 30 components describe the exact curve with excellent accuracy except close to the boundaries. This discrepancy is of course due to the unrealistic boundary condition of a vanishing vertical derivative at the top and at the bottom of the atmospheric column. Fig. 4 shows that a quite good approximation is obtained with only 5 vertical structure functions. This is important, because only relatively few components may be computed realistically from the standard isobaric surfaces.

REFERENCES

- Charney, J. G., 1947. The dynamics of the long waves in a baroclinic westerly current, *J. of Meteor.*, **4**, 135-162.
- Charney, J. G., 1973. Planetary fluid dynamics. *Dynamic Meteorology* (Ed. P. Morel), Reidel Publ. Co., 99-351.
- Chen, T. -C. and A. Wiin-Nielsen, 1978. On the nonlinear cascades of atmospheric energy and enstrophy in a two-dimensional spectral index. *Tellus*, **30**, 313-322.
- Fjørtoft, R., 1953. On the changes in the spectral distribution of the kinetic energy for the two-dimensional, nondivergent flow. *Tellus*, **5**, 225-230.
- Gates, W. L., 1961. Static stability measures in the atmosphere, *J. Meteor.*, **18**, 526-533.

- Jacobs, S. J. and A. Wiin-Nielsen, 1966. On the stability of a barotropic, basic flow in a stratified atmosphere. *J. Meteor.*, **23**, 682-687.
- Platzman, G. W., 1960. The spectral form of the vorticity equation. *J. Meteor.*, **17**, 635-644.
- Saltzman, B. and A. Fleisher, 1960. The exchange of kinetic energy between larger scales of atmospheric motion. *Tellus*, **12**, 374-377.
- Saltzman, B. and S. Teweles, 1964. Further statistics on the exchange of kinetic energy between hamonic components of the atmospheric flow. *Tellus*, **16**, 432-435.
- Steinberg, H. L., A. Wiin-Nielsen and C. -H. Yang, 1971. On nonlinear cascades in large-scale atmospheric flow. *J. Geophys. Res.*, **76**, 8629-8640.
- Wiin-Nielsen, A., 1985. The scientific problem of medium-range weather prediction. Proc. of seminar to commemorate the 10 anniv. of ECMWF., 31-53.
- Wiin-Nielsen, A. and H. Marshall, 1990. Part III. On the structure of transient atmospheric waves. *Atmósfera*, **3**, 73-109.
- Yang C. -H., 1967. Non-linear aspects of the large-scale motion in the atmosphere, Ph.D. thesis, Univ. of Mich., 173 pp.